Am J Transl Res 2013;5(5):510-520
www.ajtr.org /ISSN:1943-8141/AJTR1306006

Original Article

Chemotaxis of human induced pluripotent stem cell-derived endothelial cells

Ngan F Huang[1,2,3], Ruby E Dewi[4], Janet Okogbaa[1], Jerry C Lee[1], Abdul JalilRufaihah[1], Sarah C Heilshorn[4], John P Cooke[1,2]

[1]Division of Cardiovascular Medicine, Stanford University, 300 Pasteur Drive, Stanford, CA 94305-5406, USA; [2]Stanford Cardiovascular Institute, Stanford University, 300 Pasteur Drive, Stanford, CA 94305, USA; [3]Center for Tissue Regeneration, Repair and Restoration, Veterans Affairs Palo Alto Health Care System, 3801 Miranda Avenue, Palo Alto, CA 94304, USA; [4]Department of Materials Science and Engineering, Stanford University, 476 Lomita Mall, Stanford, CA 94305, USA

Received June 28, 2013; Accepted July 15, 2013; Epub August 15, 2013; Published August 30, 2013

Abstract: This study examined the homing capacity of human induced pluripotent stem cell-derived endothelial cells (iPSC-ECs) and their response to chemotactic gradients of stromal derived factor-1α (SDF). We have previously shown that EC derived from murine pluripotent stem cells can home to the ischemic hindlimb of the mouse. In the current study, we were interested to understand if ECs derived from human induced pluripotent stem cells are capable of homing. The homing capacity of iPSC-ECs was assessed after systemic delivery into immunodeficient mice with unilateral hindlimb ischemia. Furthermore, the iPSC-ECs were evaluated for their expression of CXCR4 and their ability to respond to SDF chemotactic gradients *in vitro*. Upon systemic delivery, the iPSC-ECs transiently localized to the lungs but did not home to the ischemic limb over the course of 14 days. To understand the mechanism of the lack of homing, the expression levels of the homing receptor, CXCR4, was examined at the transcriptional and protein levels. Furthermore, their ability to migrate in response to chemokines was assessed using microfluidic and scratch assays. Unlike ECs derived from syngeneic mouse pluripotent stem cells, human iPSC-ECs do not home to the ischemic mouse hindlimb. This lack of functional homing may represent an impairment of interspecies cellular communication or a difference in the differentiation state of the human iPSC-ECs. These results may have important implications in therapeutic delivery of iPSC-ECs.

Keywords: Induced pluripotent stem cells, endothelial cells, CXCR4, SDF-1, homing, hindlimb ischemia

Introduction

Ischemic cardiovascular diseases are a leading cause of death and disability in the United States [1]. Included in this category is peripheral arterial disease (PAD), affecting over 8 million people in the US [2]. Usually due to atherosclerotic occlusive disease of the limb arteries, PAD causes intermittent claudication, ulceration, and gangrene. A key feature of PAD is dysfunction or damage to the vascular endothelial cells (ECs) that regulate vascular tone, remodeling and angiogenesis. Despite the benefits of pharmacotherapy or interventional approaches, improved therapies for PAD are needed. Cell-based approaches to revascularize ischemic tissues are a promising approach. Although adult stem cell therapy has shown moderate improvement in limb perfusion and walking distance, a major limitation is the reduced number and impaired function of adult stem cells in patients with age and other cardiovascular risk factors [3, 4].

We have previously demonstrated that human induced pluripotent stem cells (iPSCs) are a potential source of autologous ECs for repair of PAD. We have found that iPSC-derived ECs (iPSC-ECs) manifest both the phenotype and function of mature ECs [5]. In mice with experimentally induced hindlimb ischemia, the locally injected iPSC-ECs enhanced limb perfusion, incorporated into existing vasculature, and secreted angiogenic factors that promoted endogenous vessel formation [6].

In the current study, we were interested to extend our characterization of human iPSC-ECs by assessing their capacity to home to ischemic tissue. Previously, we observed that systemically delivered syngenic murine embryonic stem cell-derived ECs (ESC-ECs) were capable of homing to the site of ischemia after femoral artery ligation [7]. If human iPSC-ECs were also capable of homing, this would make therapeutic application more feasible, by permitting intravenous delivery.

Chemokines, including those comprising the CXC family, enhance angiogenesis by directed cell migration along a soluble concentration gradient. Stromal derived factor-1α (SDF, also known as CXCL12) is released by stromal cells at sites of ischemia and recruits bone marrow-derived stem/progenitor cells bearing the CXCR4 receptor [8, 9]. The SDF-CXCR4 axis plays a prominent role in stem/progenitor cell trafficking, chemotaxis, engraftment, and therapeutic angiogenesis. The importance of this axis is evident in embryonic development as $CXCR^{-/-}$ null mice display abnormal branching of the mesentery vessels hemorrhaging of the small intestines, suggesting that CXCR4 is required for normal vascularization of the small intestines and mesentery branching [10]. CXCR4 appears to be indispensable as $CXCR4^{-/-}$ null mice die shortly after birth [11].

Accordingly, in this study, we investigated the homing capacity of iPSC-ECs by evaluating their response to chemotactic gradients of SDF or VEGF. We show that iPSC-ECs express CXCR4n but do not respond to SDF signaling cues *in vitro* or *in vivo*.

Materials & methods

Cell culture

Human iPSCs (HUF5) were expanded on mouse embryonic fibroblasts in standard pluripotent stem cell media containing 10 ng/ml basic fibroblast growth factor. The iPSCs were differentiated into iPSC-ECs by the formation of embryoid bodies, along with stimulation with vascular endothelial growth factor (VEGF) and bone morphogenetic protein-4 (BMP4), as described previously [6]. The iPSC-ECs were purified by fluorescence activated cell sorting (FACS) based on CD31 expression and characterized as described in our previous publications [5, 6]. Human primary microvascular ECs (HMDECs, Lonza) were cultured in EGM-2MV endothelial expansion media (Lonza). Human Jurkat T lymphocytes (ATCC) were cultured in Roswell Park Memorial Institute medium (RPMI) with 10% fetal bovine serum.

Incorporation of acetylated low density lipoprotein (ac-LDL)

To confirm endothelial identity of the iPSC-ECs, we examined their ability to incorporate ac-LDL, which is a functional characteristic of ECs. The iPSC-ECs were incubated in fluorescently labeled ac-LDL in expansion media for 8 hours, before the media was rinsed with phosphate buffered saline. The samples were then fixed in 4% paraformaldehyde and counterstained with Hoechst33342 before visualizing the samples using a Nikon Eclipse fluorescence microscope.

Immunofluorescence staining

Immunofluorescence staining of cells was carried out by fixation in 4% paraformaldehyde, followed by permeabilization in 0.5% Triton-X100, and then blocking in 1% bovine serum albumin (BSA). The primary antibodies consisted of CD31 (R&D Systems), vascular endothelial-cadherin (VE-cadherin, Santa Cruz Biotechnology), eNOS (BD Transduction Labs), and CXCR4 (R&D Systems). The primary antibodies were applied to the samples for overnight incubation, followed by incubation with Alexafluor (Invitrogen) secondary antibodies. Total nuclei were stained with Hoechst33342 (Invitrogen). Fluorescence images were acquired on a Nikon Eclipse microscope.

Immunoblotting

BCA protein assay (Pierce), polyacrylamide gel electrophoresis (SDS-PAGE) and transfer to nitrocellulose membranes were performed as previously described [12]. The nitrocellulose membranes were incubated with CXCR4 (Abnova), VE-cadherin (Abcam), or total actin (Sigma) antibodies. Horseradish peroxidase (HRP)-conjugated secondary antibodies were applied, and the proteins were visualized by an ECL Detection Kit (Amersham). Protein quantities were normalized by total actin abundance. Data was quantified using ImageJ software (NIH). Data was averaged out of 4 samples.

Gene expression

Total RNA was isolated using the RNEasy Kit (Qiagen) with modifications, as described previously [12]. First strand DNA was synthesized by Superscript II reverse transcriptase (Invitrogen), and quantitative real-time PCR using VE-cadherin, eNOS, CXCR4, and GAPDH Taqman assays (Applied Biosystems) was performed on a 7300 Real-Time PCR system (Applied Biosystems). Relative fold change gene expression was calculated using the $\Delta\Delta C_t$ method and normalized to GAPDH housekeeping gene.

FACS

Cells were dissociated using accutase (Sigma) and then passed through a 70 μm cell strainer. Cells were then blocked in 1% BSA before incubating with R-phycoerythrin (PE)-labeled CXCR4 antibody (R&D Systems). Isotype-matched Abs served as negative controls (Ebioscience). The cells were sorted using a FACS Aria (BD Biosciences) cell sorter.

Genetic modification of iPSC-ECs for bioluminescence imaging

For non-invasive tracking in vivo, the iPSC-ECs were genetically modified with a lentiviral construct encoding a ubiquitin promoter driving firefly luciferase (Fluc) and enhanced green fluorescence protein as described previously [7]. The transduced cells were purified by using FACS based on positive GFP expression and then expanded in EGM-2MV expansion media.

Systemic delivery and tracking of iPSC-ECs in vivo

C57Bl/6J mice (7-9 months old) were anesthetized under constant isoflurane. Unilateral hindlimb ischemia was induced by ligating and excising the femoral artery, as described previously [5, 13]. For systemic delivery of cells, a two-centimeter-long anterior midline cervical incision was made. The right external jugular vein (EJV) was exposed from the clavicle. Two 6-0 prolene sutures were loosely tied immediately distal to the right subclavian vein and proximal to the EJV bifurcation. The sutures were attached to hemostatic clips that could be raised, allowing the EJV to be temporarily occluded. Using a 28-gauge syringe, the bioluminescent iPSC-ECs ($5X10^5$ cells in 150 μl PBS) were injected into the EJV (n=6). Both the proximal and distal EJV were ligated immediately to prevent excessive bleeding. The incision site was then closed using 5-0 vicryl sutures. To track iPSC-EC homing and survival over the course of 14 days, D-luciferin (375 mg/kg body weight) was administered by intraperitoneal injection and animals imaged on an IVIS-Spectrum (Xenogen) machine. All animal procedures were approved by the Administrative Panel on Laboratory Animal Care at Stanford University.

Microfluidic device fabrication and chemotaxis assays

Microfluidic devices were fabricated using standard soft lithography and micro-molding techniques at the Stanford Microfluidics Foundry clean room. The devices were made by pouring polydimethyl siloxane (PDMS) (Sylgard 184 Silicone elastomer kit) onto the silicon mold and baking in the oven for 1 hour. Inlets and outlets to the cell culture chamber and reagent channels were punched using a tin-coated hole puncher, and the devices bonded irreversibly onto glass slides by treatment with oxygen plasma.

The cell culture chamber was adsorbed with fibronectin overnight (10 μg/mL) and rinsed three times with media. HMDECs or iPSC-ECs were suspended (500,000 cells/mL) in EGM-2MV, modified with reduced (5%) fetal bovine serum and without growth factor supplements. The cells were injected into the cell culture chamber, and allowed to adhere for 3 hours. By supplying media spiked with VEGF (50 ng/ml) or human SDF1α (hSDF; 125 ng/ml, Peprotech) into the source reagent channel, and assay media into the sink reagent channel (flow rate = 0.6 mL/hr), a stable linear gradient of growth factors is formed across the cell culture chamber. In some experiments, hSDF was added to the source channel at much higher concentrations of 1000 ng/ml. The stability of the linear gradient in this microfluidic device was characterized previously [14].

To track migrating cells, a time-lapse video microscopy system (Zeiss) equipped with an incubator to control temperature and CO_2 (set to 37°C and 5% CO_2 respectively) was used. Cells were imaged every 15 minutes for 24

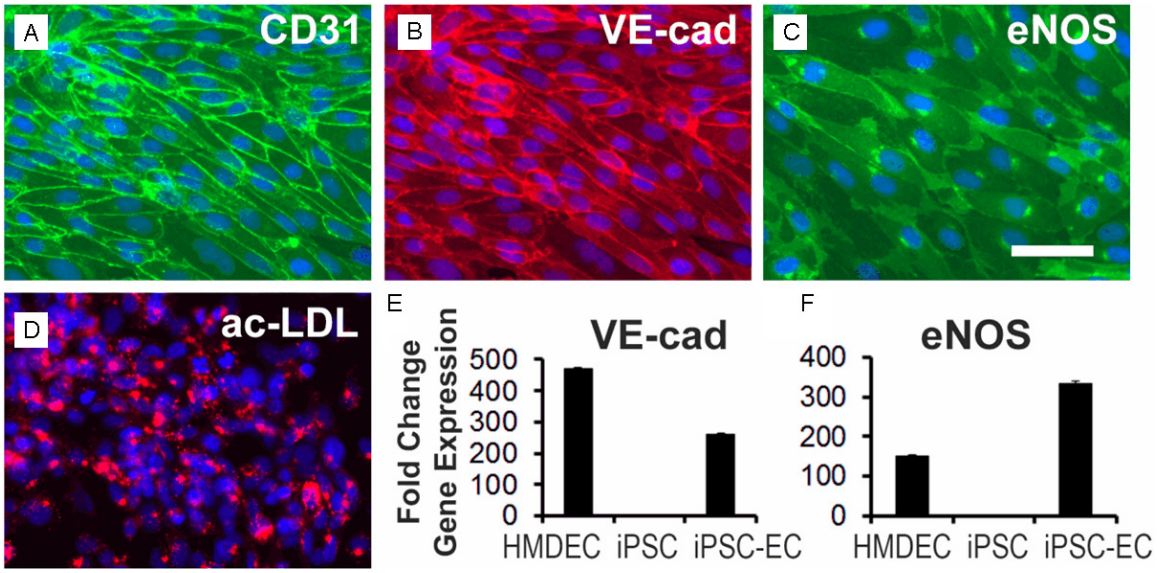

Figure 1. Characterization of iPSC-ECs. The iPSC-ECs express known endothelial markers including CD31 (A), VE-cadherin (VE-cad, B), and eNOS (C), and incorporate acetylated low density lipoprotein (ac-LDL) (D). Gene expression analysis of VE-cad (E) and eNOS (F). Scale bar: 50 μm.

hours, and tracked using ImageJ mTrackJ plugin. Cell migration was determined by tracking the center of each cell nucleus over time. Chemotactic Index was defined to be the ratio of the net distance a cell migrates in the direction of the gradient to the total length of the cell track. At least 56 cells were quantified in total for each condition.

The distribution of the chemotactic indices within each group was determined to be Gaussian using Prism (GraphPad). Directional histograms of migrating cells were generated using Chemotaxis Tool freeware (Ibidi), which generates a smoothed histogram for the number of cells migrating within a specific angular trajectory (in bins of 10°).

Wound healing scratch assay

The iPSC-ECs were cultured in EGM-2MV within silicone inserts with defined wound area (Ibidi) between two adjacent chambers. Upon confluency, the silicone chambers were detached using forceps, and the cells were switched to EGM-2MV media, modified with reduced (5%) fetal bovine serum and no growth factor supplements. VEGF (20 ng/ml), hSDF (150-500 ng/ml), or murine SDF (mSDF, 150 ng/ml, Peprotech) were then added to the media. Images of the wound area were taken at 0 and 24 hours using brightfield exposure and then analyzed for the area between edges of the wound (ImageJ). The percent scratch closure is defined as [15]:

$$Scratch\ Closure\ (\%) = [1 - \frac{Wound\ Area\ (t = 24\ h)}{Wound\ Area\ (t = 0\ h)}]X100$$

Data was averaged over four independent experiments.

Statistical analysis

Data are shown as mean ± standard deviation, unless otherwise stated. For microfluidic migration analysis, the median and interquartile ranges are shown.

Statistical analysis between multiple groups was performed by analysis of variance (ANOVA) with the Tukey adjustment. Statistical significance was accepted at $P<0.05$.

Results

Characterization of iPSC-ECs for endothelial phenotype

The iPSC-ECs have been extensively characterized in our previous publications [5, 6]. To confirm the endothelial identity of the iPSC-ECs, we showed that the iPSC-ECs uniformly express endothelial phenotypic markers CD31, VE-cadherin, and eNOS, as shown by the immuno-

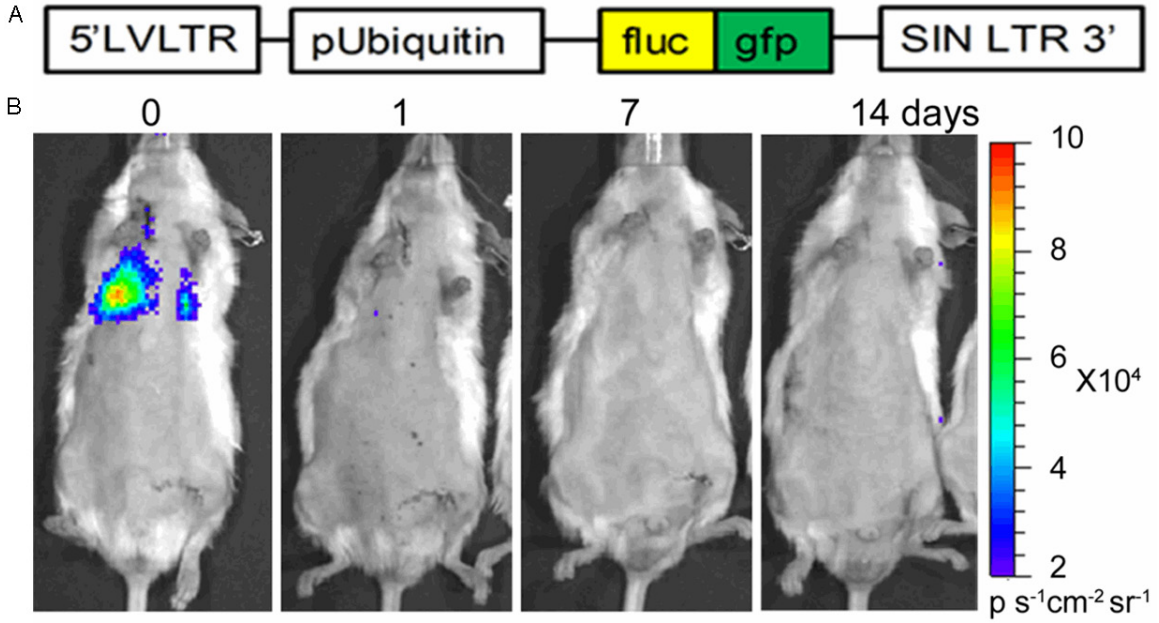

Figure 2. Localization and survival of iPSC-ECs after intravenous delivery. A. Lentiviral construct for bioluminescence imaging. B. Upon systemic delivery, the bioluminescent iPSC-ECs lodged in the lungs and did not home to the ischemic hindlimb.

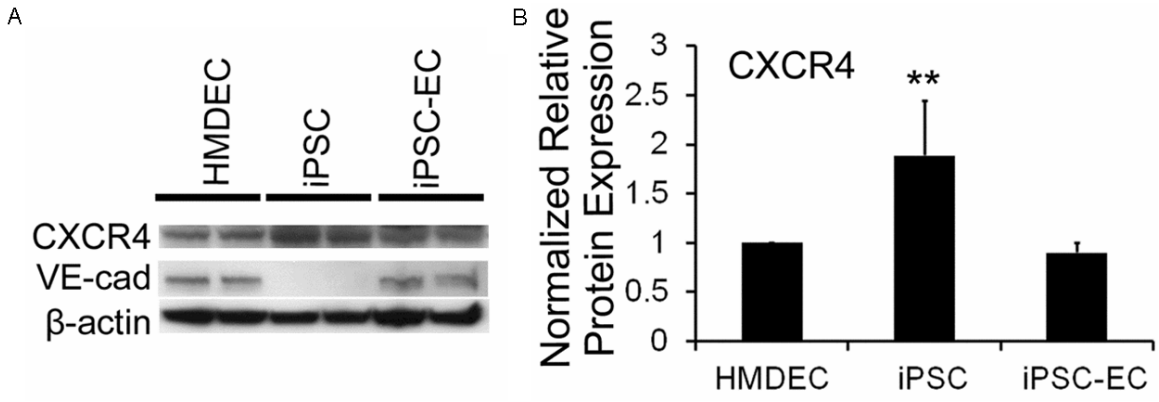

Figure 3. Protein expression of CXCR4 in HMDECs, iPSC-ECs, and parental iPSCs. A. Representative immunoblots. B. Quantification of protein expression. **<P.005.

fluorescence images in **Figure 1A-C**. Furthermore, they could incorporate ac-LDL (**Figure 1D**). We further verified the expression of VE-cadherin and eNOS at the transcriptional level by demonstrating >100-fold higher expression in iPSC-ECs, when compared to the parental iPSCs, reaching levels similar to those of HMDECs (**Figure 1E** and **1F**).

Localization and survival of systemically delivered iPSC-ECs

Based on our previous work demonstrating that murine syngenic embryonic stem cell-derived ECs (ESC-ECs) localize to the ischemic limb upon systemic delivery [7], we evaluated whether human iPSC-ECs could also home to the site of ischemic injury. We genetically modified the cells with a lentiviral construct to enable non-invasive cell tracking using bioluminescence imaging (**Figure 2A**). We and others have previously shown a linear correlation between bioluminescence intensity and cell number, which enables semi-quantification of cell numbers in vivo. Bioluminescence imaging demonstrated that, after intravenous delivery, the cells were transiently lodged in the lungs,

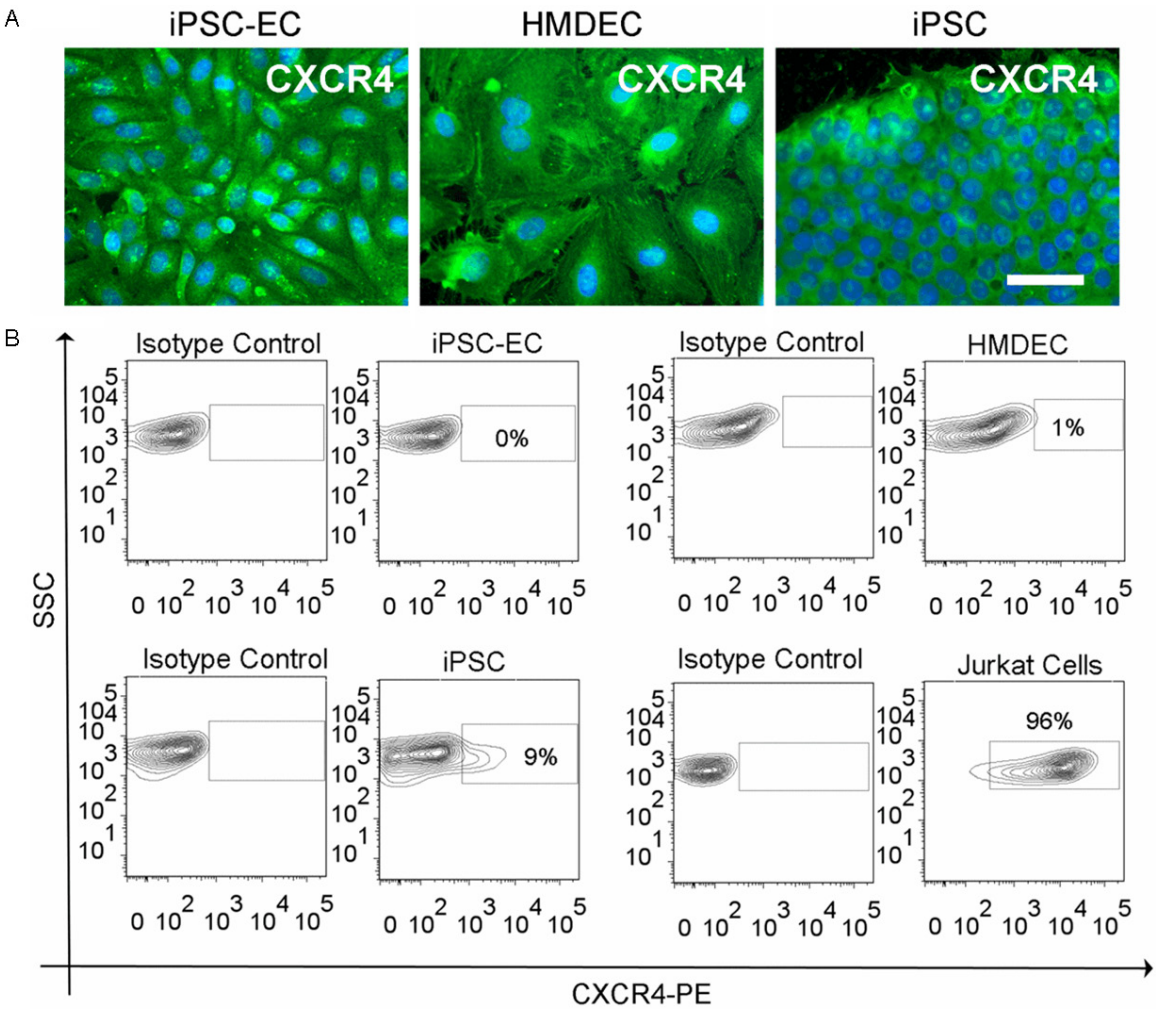

Figure 4. Localization of CXCR4. Immunofluorescence staining (A) and fluorescence activated cell sorting (B) of CXCR4. Scale bar: 50 μm.

as we had previously observed using ESC-ECs (**Figure 2B**). However, in contrast in our previous studies that demonstrated subsequent homing of murine ESC-ECs to the ischemic limb, the iPSC-ECs did not home to the ischemic limb after 14 days, and the signal over the lungs disappeared, indicating loss of viability of the injected cells.

Localization and expression of CXCR4 in iPSC-ECs

To understand the mechanism for the lack of homing capacity of human iPSC-ECs, we evaluated the expression of CXCR4, the main receptor that binds to the chemoattractant SDF. Comparison of CXCR4 at the mRNA level indicated 1000-fold reduction of CXCR4 in iPSC-ECs by comparison to HMDECs, and 100-fold reduction in comparison to the parental iPSCs (**P<0.05). Despite the significantly lower level of mRNA transcript, the protein expression of CXCR4 in the iPSC-ECs was similar to that of HMDECs (**Figure 3A** and **3B**).

To elucidate the cellular localization of CXCR4, we performed immunofluorescence staining and subsequent FACS for CXCR4. Based on immunofluorescence staining, CXCR4 was prominently expressed intracellularly within iPSC-ECs, HMDECs, as well as iPSCs (**Figure 4A**). To evaluate cell surface expression of CXCR4, we performed FACS. To our surprise, both iPSC-ECs as well as HMDECs expressed no or extremely low (1%) yields of CXCR4 on their surface (**Figure 4B**). In contrast, 96% of

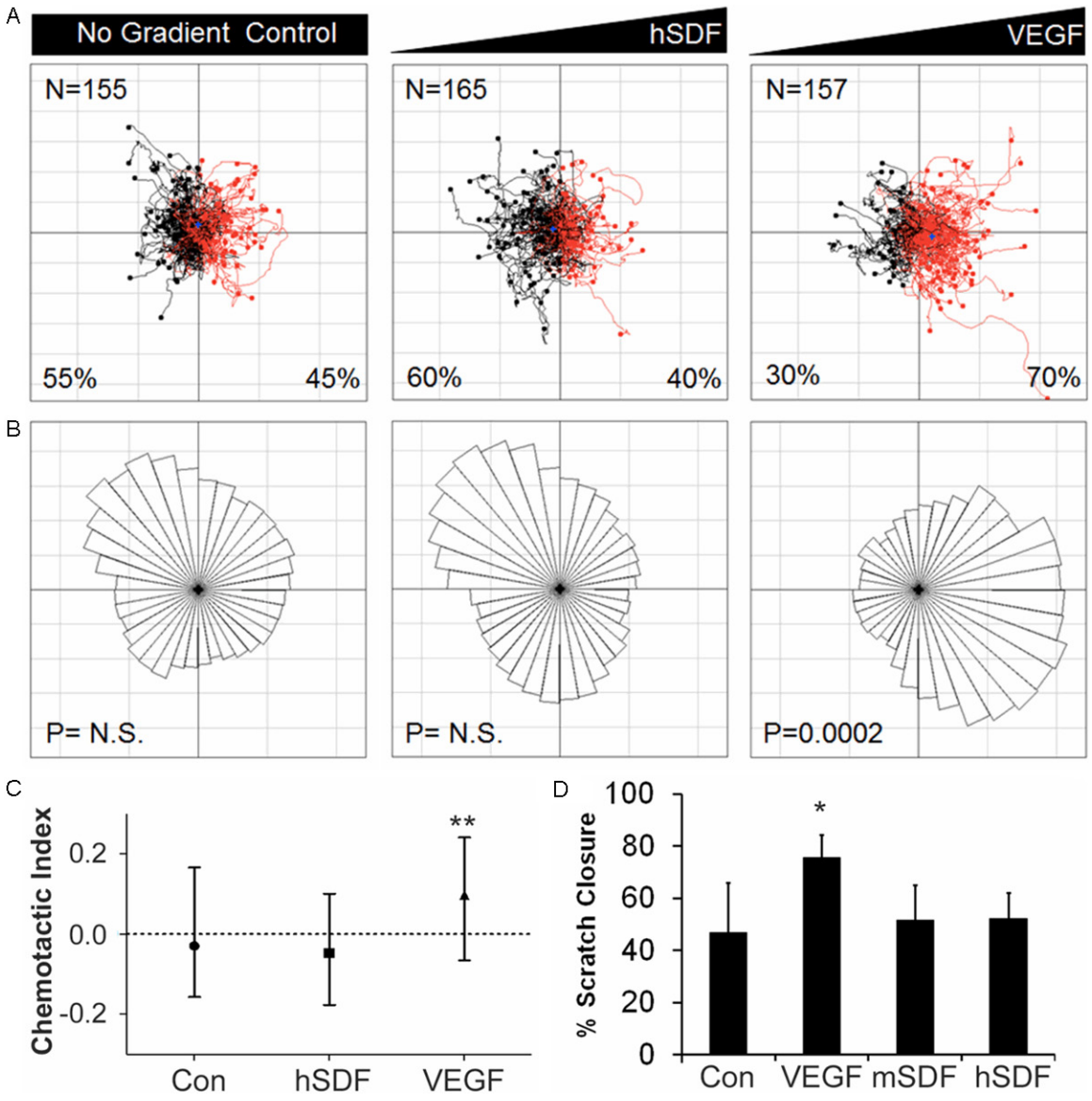

Figure 5. Chemotaxis of iPSC-EC in response to SDF and VEGF. A. Individual cell tracks are plotted, beginning from their origin (0,0). The number of cells migrating towards (red tracks) or away from (black tracks) the chemokine is given for each condition. B. Corresponding angular histogram plots. *P* values are indicated. C. Chemotactic index of iPSC-EC migration indicates chemotaxis towards VEGF (20 ng/ml) but not towards hSDF (125 ng/ml) after 24 hours. Median and interquartile range are shown. D. Scratch assay revealed enhancement of wound closure by VEGF, but not by hSDF or mSDF. **P<0.005, *P<0.05.

the Jurkat T lymphocytes (positive cell type control) showed CXCR4 expression, ruling out the possibility of technical error. The percentage of iPSCs having CXCR4 surface expression was 9%, which is consistent with the reported low expression levels found in undifferentiated pluripotent stem cells [16]. Together, these data suggested that CXCR4 intracellular protein expression was abundant in iPSC-ECs, but not on the cell surface.

Chemotactic response of iPSC-ECs to SDF gradients

Since CXCR4 is the receptor for SDF, we next determined whether the iPSC-ECs could respond to SDF chemotactic gradients. We created quantitative SDF gradients using a microfluidic device in which the SDF source channel and sink channels created a linear gradient across the cell culture chamber. Using

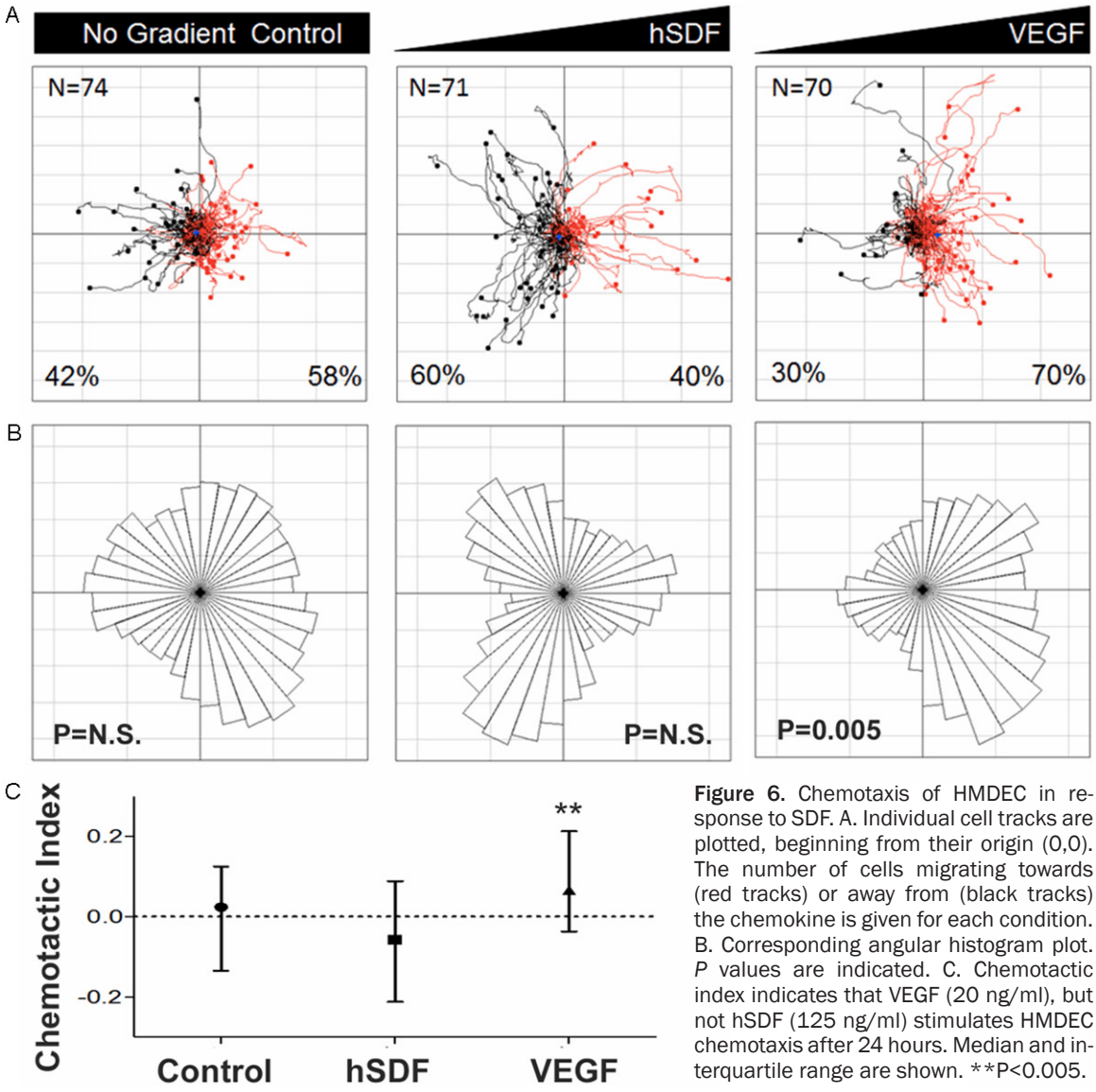

Figure 6. Chemotaxis of HMDEC in response to SDF. A. Individual cell tracks are plotted, beginning from their origin (0,0). The number of cells migrating towards (red tracks) or away from (black tracks) the chemokine is given for each condition. B. Corresponding angular histogram plot. *P* values are indicated. C. Chemotactic index indicates that VEGF (20 ng/ml), but not hSDF (125 ng/ml) stimulates HMDEC chemotaxis after 24 hours. Median and interquartile range are shown. **P<0.005.

timelapse microscopy and migration analysis software, we could quantitatively track the direction and magnitude of cell migration across the gradient. In support of our FACS and immunostaining results demonstrating the lack of CXCR4 at the cell surface, we did not observe chemotaxis in response to hSDF gradients, when compared to the negative control group in the absence of an hSDF gradient, based on cell tracking maps and their corresponding angular histogram plots (**Figure 5A** and **5B**). As a positive assay control, the chemokine VEGF did stimulate iPSC-EC migration along increasing VEGF concentrations, as is expected of ECs. We further quantified these results in the measurement of the chemotactic index as a measure of the accuracy of chemotaxis. The chemotactic indices for hSDF and the control groups were dispersed with a median value close to 0, suggesting no uniform directional movement along the concentration gradient (**Figure 5C**). In contrast, the chemotactic index for the VEGF group was +0.1, suggesting a significant directional movement up the concentration gradient (P<0.005).

We further verified these microfluidic experiments using a two-dimensional scratch assay. Here, hSDF did not statistically enhance closure of the wound (**Figure 5D**), even at higher concentration levels of 1000 ng/ml (Figure S1). By contrast, VEGF significant enhanced wound

closure ($P<0.05$). To further verify whether there may be species-related discrepancies that could account for the lack of homing of iPSC-ECs to ischemic murine tissue in vivo, we also performed similar experiments using mSDF, demonstrating that neither mSDF nor hSDF induced enhanced wound healing closure.

Chemotactic response of HMDECs to SDF gradients

Based on these data, we wondered whether the iPSC-ECs were impaired, or if the loss of homing might be a feature of more mature HMDECs. Accordingly, we utilized the same assays of chemotaxis response in HMDECs. Similar to the iPSC-ECs, the HMDECs did not migrate in response to hSDF, based on cell migration tracks and the corresponding angular histogram plots (**Figure 6A** and **6B**). In contrast to hSDF, VEGF gradients stimulated a significant chemotactic gradient in the positive direction, suggesting that VEGF promoted directional movement up the concentration gradient (**Figure 6C**).

Discussion

The salient findings of this study are: 1) iPSC-ECs express abundant CXCR4 protein intracellularly, but not on the cell surface; 2) systemically delivered iPSC-ECs did not home to the site of hindlimb ischemia *in vivo*; and 3) iPSC-ECs did not respond to chemotactic gradients of SDF using a microfluidic approach or a wound healing scratch assay. Although these responses are different than those observed in syngenic ESC-ECs, they resemble the response of mature human ECs to the same stimuli.

To date there are limited studies that have examined the expression of CXCR4 and/or SDF on pluripotent stem cell-derived ECs, and the reported results have been inconsistent. Blancas et al. reported that murine ESC-ECs did not express CXCR4 on the cell surface based on flow cytometry analysis [17]. In contrast, Chen et al. showed that the ESC-ECs expressed CXCR4 on the cell surface as well as in the intracellular space, and could respond to SDF chemotaxis by the Boyden chamber assay [18]. However, the seemingly contradictory findings between Chen et al. and the present study can be attributed to the difference in the maturation of their ESC-ECs, in comparison to our iPSC-ECs. Rather than purifying the ESC-ECs using a mature endothelial marker such as VE-cadherin, the authors selected for cells expressing a progenitor marker (CD34) that is abundantly expressed on endothelial progenitor cells and hematopoietic stem cells. After conditioning the CD34+ cells with endothelial-inducing factors, the CD34+ cells co-expressed CD31 and were termed ESC-ECs. The authors further demonstrated the plasticity of CD34+ cells to commit to hematopoietic lineages that were CD45+ and formed colony forming units in methylcellulose. Therefore, it is likely that the cell population defined by the authors as ESC-ECs are at a less mature stage than our iPSC-ECs, and thus resembled progenitor cells that may have homing capacity.

Various reports suggest that SDF-CXCR4 signaling stimulates chemotaxis of primary ECs. The biological effects begin with binding of SDF to CXCR4 or CXCR7, forming CXCR4 homodimers or CXCR4/CXCR7 heterodimers. CXCR4 is then by internalized by G-protein-coupled receptor kinases with subsequent binding of β-arrestin [19]. CXCR4 increases chemotaxis and cell survival by activating downstream signaling cascades including AKT, protein kinase C, and phosphoinositide 3-kinase [20, 21]. CXCR4 then traverses through endosomes before being recycled back to the cell surface.

Normal human ECs express CXCR4 at the transcriptional and protein levels, and could respond to SDF chemotactic gradients [22-24]. In contrast, we observed abundant intracellular, but not cell surface protein expression. Furthermore, our HDMECs did not respond to SDF but responded to VEGF with chemotaxis as expected. The cytoplasmic localization of CXCR4 in the iPSC-ECs suggests receptor internalization. One potential mediator of this process in iPSC-ECs is CXCR7, which is known to negatively regulate CXCR4 expression by affecting downstream signaling pathways as well as by blocking CXCR4 binding to SDF [25]. CXCR7 and its agonists induce CXCR4 internalization and subsequent degradation [26, 27]. Therefore, it is possible that CXCR7 may be highly expressed in both the iPSC-ECs as well as HMDECs, leading to a reduction in CXCR4 cell surface receptor as well as sequestration of SDF away from CXCR4.

In summary, we have demonstrated that systemically delivered iPSC-ECs failed to home to the site of tissue ischemia. This is in contrast to previous results using murine ECs derived from syngenic ESCs. Unlike ECs derived from syngeneic mouse pluripotent stem cells, human iPSC-ECs do not home to the ischemic mouse hindlimb. This lack of functional homing may represent an impairment of interspecies cellular communication or a difference in the differentiation state of the human iPSC-ECs. These results may have important implications in therapeutic delivery of iPSC-ECs.

Acknowledgements

This study was supported by grants from the National Institutes of Health, Bethesda, MD, to JPC (U01HL100397), NFH (HL098688), and SCH (1R21AR06235901, 1DP20D006477, 1R01DK0085720). The authors declare that they have no competing financial interests and no relationship with industry.

Disclosure of conflict of interest

None.

Address correspondence to: Dr. John P Cooke, Division of Cardiovascular Medicine, Stanford University, 300 Pasteur Drive, Stanford, CA 94305-5406, USA. Tel: 650-723-6459; Fax: 650-723-8392; E-mail: jcooke@stanford.edu

References

[1] Go AS, Mozaffarian D, Roger VL, Benjamin EJ, Berry JD, Borden WB, Bravata DM, Dai S, Ford ES, Fox CS, Franco S, Fullerton HJ, Gillespie C, Hailpern SM, Heit JA, Howard VJ, Huffman MD, Kissela BM, Kittner SJ, Lackland DT, Lichtman JH, Lisabeth LD, Magid D, Marcus GM, Marelli A, Matchar DB, McGuire DK, Mohler ER, Moy CS, Mussolino ME, Nichol G, Paynter NP, Schreiner PJ, Sorlie PD, Stein J, Turan TN, Virani SS, Wong ND, Woo D and Turner MB. Heart Disease and Stroke Statistics--2013 Update: A Report From the American Heart Association. Circulation 2013; 127: e6-e245.

[2] WRITING GROUP MEMBERS, Lloyd-Jones D, Adams RJ, Brown TM, Carnethon M, Dai S, De Simone G, Ferguson TB, Ford E, Furie K, Gillespie C, Go A, Greenlund K, Haase N, Hailpern S, Ho PM, Howard V, Kissela B, Kittner S, Lackland D, Lisabeth L, Marelli A, McDermott MM, Meigs J, Mozaffarian D, Mussolino M, Nichol G, Roger VL, Rosamond W, Sacco R, Sorlie P, Roger VL, Thom T, Wasserthiel-Smoller S, Wong ND, Wylie-Rosett J; American Heart Association Statistics Committee and Stroke Statistics Subcommittee. Heart disease and stroke statistics--2010 update: a report from the American Heart Association. Circulation 2010; 121: e46-e215.

[3] Hoetzer GL, Van Guilder GP, Irmiger HM, Keith RS, Stauffer BL and DeSouza CA. Aging, exercise, and endothelial progenitor cell clonogenic and migratory capacity in men. J Appl Physiol 2007; 102: 847-852.

[4] Vasa M, Fichtlscherer S, Aicher A, Adler K, Urbich C, Martin H, Zeiher AM and Dimmeler S. Number and migratory activity of circulating endothelial progenitor cells inversely correlate with risk factors for coronary artery disease. Circ Res 2001; 89: E1-7.

[5] Rufaihah AJ, Huang NF, Kim J, Herold J, Volz KS, Park TS, Lee JC, Zambidis ET, Reijo-Pera R and Cooke JP. Human induced pluripotent stem cell-derived endothelial cells exhibit functional heterogeneity. Am J Transl Res 2013; 5: 21-35.

[6] Rufaihah AJ, Huang NF, Jame S, Lee JC, Nguyen HN, Byers B, De A, Okogbaa J, Rollins M, Reijo-Pera R, Gambhir SS and Cooke JP. Endothelial cells derived from human iPSCS increase capillary density and improve perfusion in a mouse model of peripheral arterial disease. Arterioscler Thromb Vasc Biol 2011; 31: e72-79.

[7] Huang NF, Niiyama H, Peter C, De A, Natkunam Y, Fleissner F, Li Z, Rollins MD, Wu JC, Gambhir SS and Cooke JP. Embryonic stem cell-derived endothelial cells engraft into the ischemic hindlimb and restore perfusion. Arterioscler Thromb Vasc Biol 2010; 30: 984-991.

[8] Yamaguchi J, Kusano KF, Masuo O, Kawamoto A, Silver M, Murasawa S, Bosch-Marce M, Masuda H, Losordo DW, Isner JM and Asahara T. Stromal cell-derived factor-1 effects on ex vivo expanded endothelial progenitor cell recruitment for ischemic neovascularization. Circulation 2003; 107: 1322-1328.

[9] Christopherson KW 2nd, Cooper S and Broxmeyer HE. Cell surface peptidase CD26/DPPIV mediates G-CSF mobilization of mouse progenitor cells. Blood 2003; 101: 4680-4686.

[10] Tachibana K, Hirota S, Iizasa H, Yoshida H, Kawabata K, Kataoka Y, Kitamura Y, Matsushima K, Yoshida N, Nishikawa S, Kishimoto T and Nagasawa T. The chemokine receptor CXCR4 is essential for vascularization of the gastrointestinal tract. Nature 1998; 393: 591-594.

[11] Nagasawa T, Hirota S, Tachibana K, Takakura N, Nishikawa S, Kitamura Y, Yoshida N, Kikutani H and Kishimoto T. Defects of B-cell lym-

phopoiesis and bone-marrow myelopoiesis in mice lacking the CXC chemokine PBSF/SDF-1. Nature 1996; 382: 635-638.
[12] Yu J, Huang NF, Wilson KD, Velotta JB, Huang M, Li Z, Lee A, Robbins RC, Cooke JP and Wu JC. nAChRs mediate human embryonic stem cell-derived endothelial cells: proliferation, apoptosis, and angiogenesis. PLoS One 2009; 4: e7040.
[13] Niiyama H, Huang NF, Rollins MD and Cooke JP. Murine model of hindlimb ischemia. J Vis Exp 2009; 23: 1035.
[14] Shamloo A, Ma N, Poo MM, Sohn LL and Heilshorn SC. Endothelial cell polarization and chemotaxis in a microfluidic device. Lab Chip 2008; 8: 1292-1299.
[15] Loughlin DT and Artlett CM. Modification of collagen by 3-deoxyglucosone alters wound healing through differential regulation of p38 MAP kinase. PLoS One 2011; 6: e18676.
[16] Guo Y, Hangoc G, Bian H, Pelus LM and Broxmeyer HE. SDF-1/CXCL12 enhances survival and chemotaxis of murine embryonic stem cells and production of primitive and definitive hematopoietic progenitor cells. Stem Cells 2005; 23: 1324-1332.
[17] Blancas AA, Wong LE, Glaser DE and McCloskey KE. Specialized Tip/Stalk-Like and Phalanx-Like Endothelial Cells from Embryonic Stem Cells. Stem Cells Dev 2013; 22: 1398-407.
[18] Chen T, Bai H, Shao Y, Arzigian M, Janzen V, Attar E, Xie Y, Scadden DT and Wang ZZ. Stromal cell-derived factor-1/CXCR4 signaling modifies the capillary-like organization of human embryonic stem cell-derived endothelium in vitro. Stem Cells 2007; 25: 392-401.
[19] Zaruba MM and Franz WM. Role of the SDF-1-CXCR4 axis in stem cell-based therapies for ischemic cardiomyopathy. Expert Opin Biol Ther 2010; 10: 321-335.
[20] Ratajczak MZ, Zuba-Surma E, Kucia M, Reca R, Wojakowski W and Ratajczak J. The pleiotropic effects of the SDF-1-CXCR4 axis in organogenesis, regeneration and tumorigenesis. Leukemia 2006; 20: 1915-1924.
[21] Petit I, Goichberg P, Spiegel A, Peled A, Brodie C, Seger R, Nagler A, Alon R and Lapidot T. Atypical PKC-zeta regulates SDF-1-mediated migration and development of human CD34+ progenitor cells. J Clin Invest 2005; 115: 168-176.
[22] Feil C and Augustin HG. Endothelial cells differentially express functional CXC-chemokine receptor-4 (CXCR-4/fusin) under the control of autocrine activity and exogenous cytokines. Biochem Biophys Res Commun 1998; 247: 38-45.
[23] Salcedo R, Wasserman K, Young HA, Grimm MC, Howard OM, Anver MR, Kleinman HK, Murphy WJ and Oppenheim JJ. Vascular endothelial growth factor and basic fibroblast growth factor induce expression of CXCR4 on human endothelial cells: In vivo neovascularization induced by stromal-derived factor-1alpha. Am J Pathol 1999; 154: 1125-1135.
[24] Gupta SK, Lysko PG, Pillarisetti K, Ohlstein E and Stadel JM. Chemokine receptors in human endothelial cells. Functional expression of CXCR4 and its transcriptional regulation by inflammatory cytokines. J Biol Chem 1998; 273: 4282-4287.
[25] Levoye A, Balabanian K, Baleux F, Bachelerie F and Lagane B. CXCR7 heterodimerizes with CXCR4 and regulates CXCL12-mediated G protein signaling. Blood 2009; 113: 6085-6093.
[26] Naumann U, Cameroni E, Pruenster M, Mahabaleshwar H, Raz E, Zerwes HG, Rot A and Thelen M. CXCR7 functions as a scavenger for CXCL12 and CXCL11. PLoS One 2010; 5: e9175.
[27] Uto-Konomi A, McKibben B, Wirtz J, Sato Y, Takano A, Nanki T and Suzuki S. CXCR7 agonists inhibit the function of CXCL12 by down-regulation of CXCR4. Biochem Biophys Res Commun 2013; 431: 772-776.

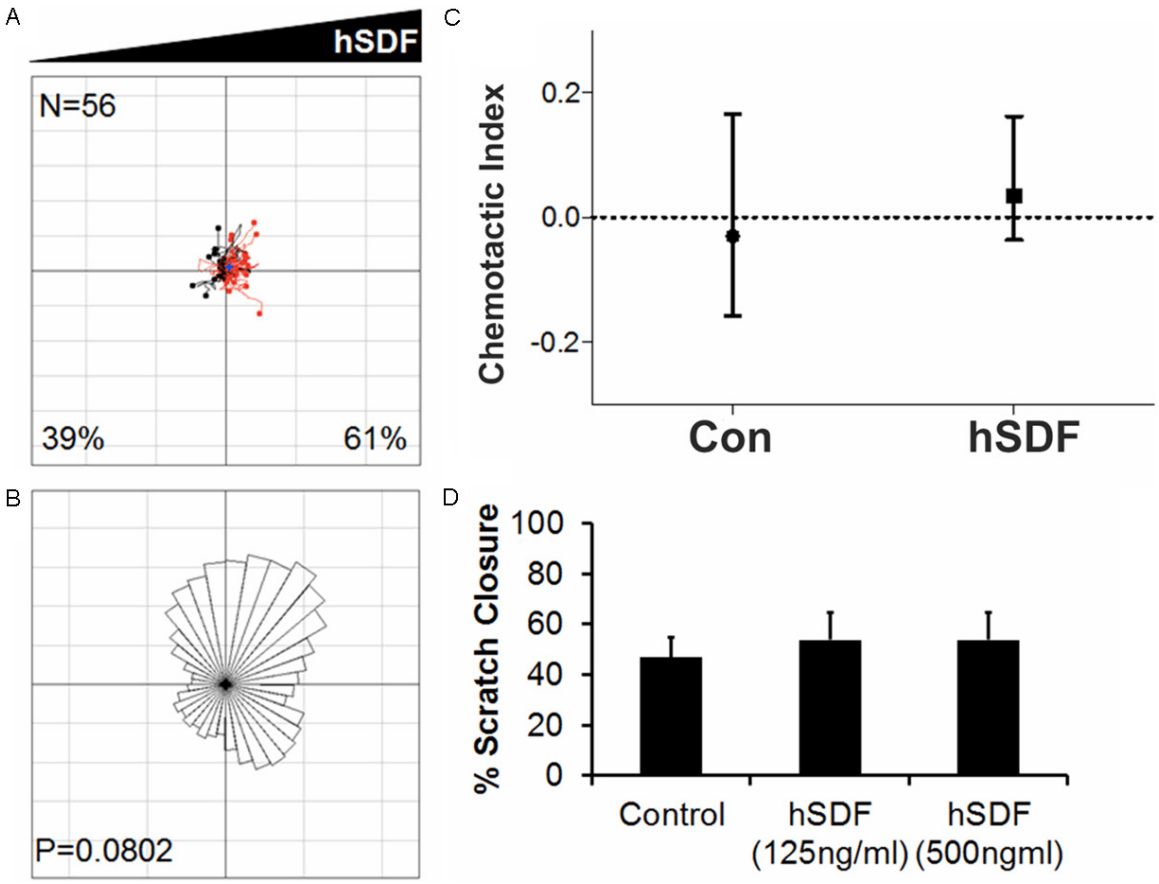

Figure S1. Lack of chemotaxis to high dose SDF. A. Individual cell tracks are plotted, beginning from their origin (0,0). The number of cells migrating towards (red tracks) or away from (black tracks) the chemokine is given for each condition. B. Corresponding angular histogram plot. *P* values are indicated. C. Chemotactic index indicates lack of chemotaxis towards hSDF (500 ng/ml) after 24 hours. Median and interquartile range are shown. D. Confirmation by scratch assay that hSDF does not stimulate chemotaxis in iPSC-EC.